Robustness Analysis Under Second-Order Plant and Delay Uncertainties for Symmetrically Coupled Systems with Time Delay

Joono Cheong*
Department of Control and Instrumentation Engineering, Korea University, Jochiwon, Chungnam 339-700, Korea
SangJoo Kwon
School of Aerospace and Mechanical Engineering, Hankuk Aviation University (HAU), Goyang, Kyunggi 412-791, Korea

This paper aims at presenting robustness analysis under the uncertainties of the time delay and plant parameters in symmetrically coupled dynamic systems connected through network having time delay. The delay-involved closed loop characteristic function is mathematically formulated, incorporated with active synchronization control. And the robust stability of the corresponding system is analyzed by investigating the formation of characteristic equation containing second-order terms of uncertainty variables representing delay and plant dynamics mismatches. For the two individual types of uncertainties, we elucidate details of how to compute the bounds and what they imply physically. To support the validity of the mathematical claims, numerical examples and simulations are presented.

Key Words : Uncertainty, Time Delay, Synchronization, Coupled System

1. Introduction

Coupled systems accommodate multiple subsystems connected through some ways of communication. Position matching between subsystems within a coupled system implies a task of synchronizing position state among the subsystems in different locations. If the distance between the subsystems is large, information exchange may take non-negligible time, which necessitates time-delay consideration in the characterization of closed loop behavior. Broad range of synchronization controls for coupled systems can be found in various literatures in engineering fields, no matter if time delay is considered or not.

A variety of master-slave systems in the teleoperator control are representative examples that hold ideal requirements of perfect position synchronization as well as transparency (Aderson and Spong, 1989; Niemeyer and Slotine, 1991; Lawrence, 1993) under communication delay, though both cannot be achieved simultaneously. Control of identical dual-cylinder electro-hydraulic lift system (Sun and Chiu, 2002) is another example of synchronization addressed by Sun and Chiu. Generalized synchronization control to multi-axis identical motion control systems was also studied in (Liu and Sun, 2005), where the stabilization issue was mainly addressed. A synchronization approach to minimize the mutual error between mobile vehicle and loaded manipulator was reported in (Sun and Feng, 2003; Rodriguez-Angeles and Nijmeijer, 2004). An Internet based model predictive control approach (Changhong et al., 2004) was used to synchronize remote plant and local computer model, where

* Corresponding Author,
E-mail : jncheong@korea.ac.kr
TEL : +82-41-860-1449; **FAX** : +82-41-865-1820
Department of Control and Instrumentation Engineering, Korea University, Jochiwon, Chungnam 339-700, Korea. (Manuscript **Received** December 29, 2005; **Revised** June 5, 2006)

the randomness of time delay was explicitly dealt with. In shared virtual environment applications, a position synchronization scheme was introduced (Cheong et al., 2005) to allow multiple users to interact through shared virtual objects in the distributed virtual environment.

Not only the stability analysis, but also the robustness analysis is very much important in the synchronization control with time delay. Since time delay plays a severely adverse role in the stability point of view, special care must be paid to delay uncertainty. In the work done by Yamanaka and Shimemura (1987), a necessary and sufficient robust stability condition was addressed under the plant and time delay uncertainties using the frequency sweeping technique. This was derived from comparing the growth rate of plant uncertainty in the high frequency and designed controller using Smith predictor (Smith, 1957; Satacesaria and Scattolini, 1993). Uncertainty in the delay was specially considered in (Zhang and Xu, 2001), where it is suggested that a suitable choice of controller order can improve performance and the uncertainty bound as well. In the case of teleoperator control systems, the uncertainty in the plant was considered during the synthesis of robust controller using like H_∞ or μ-synthesis (Kazerooni et al., 1993; Lung et al., 1995) frameworks. However, such design methods have not clearly shown ways to handle time delay uncertainty, which possibly limits the applicability in practice. Taoutaou et al.(2003) performed a robustness analysis for a eleoperator system under time delay and plant uncertainties by explicitly deriving the characteristic function in terms of dynamic parameters.

In this paper we particularly focus on the robustness issue in coupled systems where identical subsystems are connected with communication delay. In such cases, total uncertainty effect comes from the combination of uncertainty portion from each subsystem because the overall transfer function is obtained by the multiplication of each subsystem. When n number of identical subsystems is contained in an overall coupled system, the characteristic function bears higher-order terms of an uncertainty variable such that

$$p_n(s)\,\delta^n(s)+p_{n-1}(s)\,\delta^{n-1}(s)+\cdots+p_0(s)$$

where $p_i(s)$, $i=0, 1, \cdots, n$ is a polynomial, and $\delta(s)$ is the uncertainty portion from a single subsystem. This implies that we need to derive a condition of robust bound of $\delta(s)$ from this higher-order polynomial characteristic equation. This is the issue to be discussed in the paper that has rarely been presented in control community, to the authors' best knowledge. If we follow the conventional formation of uncertainty where only a single lumped uncertainty is considered, very fine tuning of uncertainty bound in each subsystem may not be possible.

The organization of the rest of the paper is as follows. Section 2 explains preliminary definitions and notations, section 3 presents main results on robustness analysis, and section 4 illustrates simulation results. Finally, summary and concluding remarks are made in section 5.

2. System Description

We consider a symmetrically coupled system in Fig. 1 that consists of two identical subsystems at site 1 and site 2 connected via communication channel. There exists time delay for data communication between the two sites. An elementary requirement is that for arbitrary smooth and bounded local input, F_i, $i=1, 2$, the two subsystems are to be synchronized even with time-delay, so that each subsystem has the same or very close state (i.e., position and velocity) for all time. This synchronization requirement can be attained by using a feedback controller which is capable of compensating for any possible de-synchronization error, caused by model mismatch, numerical error, or data loss in the course of communication.

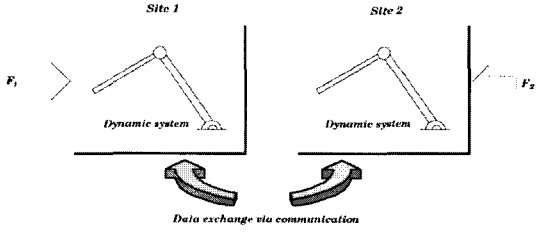

Fig. 1 Schematic of generic coupled systems

A notable approach for the synchronization between two subsystems is to use two-way Smith predictor scheme proposed by Cheong et al.(2005) shown in Fig. 2, which is effective when plant model and delay are known precisely. This scheme achieves stability and performance simply by tuning a controller, $K(s)$. We will consider the structure in Fig. 2 as the primary setting for the symmetrically coupled systems in this paper — however, the subsequent analysis can be equally applicable to other forms of controllers. Originally this scheme was introduced for synchronizing shared virtual environment and enabling immediate responsiveness and state consistency[1]. For details, refer to (Cheong et al., 2005) and references therein. Although, however, the scheme in Fig. 2 can be adapted to synchronizing coupled systems in general class of robotics and control applications, uncertainties in these practical systems may deteriorate the control performance and even destabilize the overall system. Hence, it is necessary to investigate the robustness properties of the overall system combined with the proposed scheme, in order to extend the feasibility of the scheme to a variety of applications. Implementation issues like control input saturation may be also important in practice but these will not be treated in this paper.

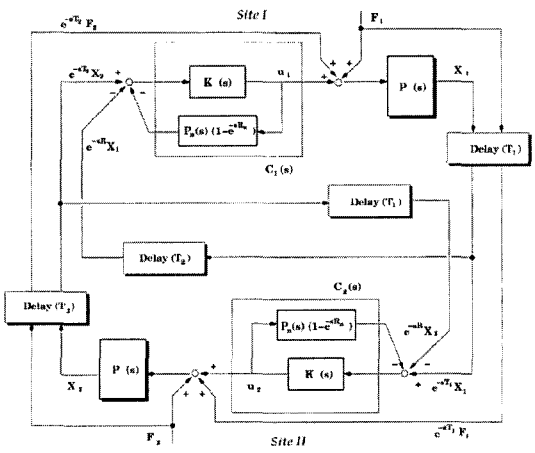

Fig. 2 Structure of motion synchronization control scheme

As a preliminary, this section is devoted to descriptions of main equations and definitions that characterize the overall control system. For the time being, we do not consider uncertainties in the controller, that is, $P_n(s)=P(s)$ and $R_n=R$. Assume $P(s)$ is a second order linear system having a damping resistance such that

$$p(s)=\frac{1}{ms^2+bs} \tag{1}$$

where m and b denote physical mass and damping coefficients, respectively. Other types of physical properties may be included such as stiffness terms. However, we mainly consider the case of unconstrained motion without spring-like constraint. (Actually existence of stiffness term works favorably to state synchronization.) External inputs to the system are F_1 and F_2, which are smooth and have bounded energy, applied to plants at site 1 and site 2, respectively. Sum of two unilateral delays, T_1 and T_2, which represent delays from site 1 to site 2, and from site 2 to site 1, respectively, makes total round trip delay, R, that is, $R=T_1+T_2$.

As shown in Fig. 2, the controller, $C_i(s)$, compensates for skewed error between the sites by comparing states delivered over the network. Note that it has a fully symmetrical structure, so that there is no concept of master or slave as in teleoperator control. To be precise, it gives an equal chance to every participating user at each site. So it might be applicable to multi-user haptic simulation, expert-learner skill teaching systems, or many general synchronization systems that need n-independent users. Readers may find more background information about the control structure from reference (Cheong et al., 2005). The whole control structure consists of a primary controller, $K(s)$, and a Smith predictor based internal model, $P_n(s)-P_n(s)e^{-sR_n}$. The primary controller, $K(s)$, adopts simple PD action, that is, of the form, $K(s)=k_v s+k_p$, where k_v and k_p are velocity and proportional gains, respectively. Smith predictor based internal model estimates current state and previous state delayed by time

1) Responsiveness is the ability of how fast the response is produced from input, and consistency implies the condition when every participating site has the same virtual environment state at the same instance.

unit R with precise knowledge of plant dynamics and amount of time delay. If the estimation is perfect, there will be exact cancelation between the estimated and actual feedback signal delayed by R, resulting in that the overall feedback system eventually becomes a new one that has immediate feedback and performs with desired specification at a desired level. Refer to (Smith, 1957; Niculescu, 2001) for more information on Smith predictor. Discrete-time implementation of Smith predictor based estimation is done by a stack of buffer that stores a sequence of estimated current state along with time stamps as shown in Fig. 3. Also note that, since the current system has a symmetric placement of Smith predictors, we call it a two-way Smith predictor structure.

Now, since $P_n(s)=P(s)$ and $R_n=R$, the following algebraic equations are obtained from the structure in Fig. 2.

$$u_i=\frac{K(s)}{1+K(s)P(s)(1-e^{-sR})}(X_j e^{-sT_j}-X_i e^{-sR}) \quad (2)$$

$$X_i=P(s)(u_i+F_j e^{-sT_j}+F_i) \quad (3)$$

for $i, j=1, 2$, and $i\neq j$, where u_i is the control input to $P(s)$. Substituting (3) into (2) and performing simple algebraic manipulation, we get a transfer relation as

$$\begin{bmatrix}X_1\\X_2\end{bmatrix}=\frac{1}{\varphi(s,R)}\begin{bmatrix}h_{11}(s) & h_{12}(s)\\h_{21}(s) & h_{22}(s)\end{bmatrix}\begin{bmatrix}F_1\\F_2\end{bmatrix} \quad (4)$$

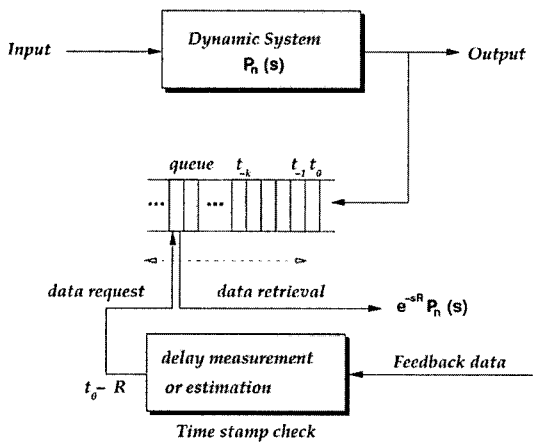

Fig. 3 Discrete-time implementation of Smith predictor

where $\varphi(s,\delta R)$ is the characteristic function given by

$$\begin{aligned}\varphi(s,\delta R)&=\alpha_1(s)+\alpha_{2(s)}e^{-sR}\\&=(M(s)+K(s))^2-K^2(s)e^{-sR}\end{aligned} \quad (5)$$

and

$$h_{11}(s)=\frac{(M(s)+K(s))(M(s)+(1-e^{-sR})K(s))}{M(s)}$$

$$h_{12}(s)=e^{-sT_2}\frac{K(s)(M(s)+(1-e^{-sR})K(s))}{M(s)}$$

$$h_{21}(s)=e^{-sT_1}\frac{K(s)(M(s)+(1-e^{-sR})K(s))}{M(s)}$$

$$h_{22}(s)=\frac{(M(s)+K(s))(M(s)+(1-e^{-sR})K(s))}{M(s)}$$

where $M(s):=ms^2+bs$. As is well known, there are three types of delay systems depending on the relative degrees of $\alpha_1(s)$ and $\alpha_2(s)$ in (5). That is, (i) if $\deg[\alpha_1(s)]>\deg[\alpha_2(s)]$, it is a retarded type, (ii) if $\deg[\alpha_1(s)]=\deg[\alpha_2(s)]$, it is neutral, and (iii) otherwise, it is an advanced type. In a retarded type system, if all the roots of $\varphi(s,0)$ lie in the left half complex plane, then all the new zeros of $\varphi(s,R)$ for infinitesimal nonzero R still lie in the left half plane. Hence, for such a type, the stability is a matter of finding maximal R for which any zero of $\varphi(s,R)$ is in the imaginary axis as R is gradually increased. Refer to references such as (Walton and Marshall, 1987; Niculescu, 2001; Bellman and Cooke, 1963) for introductions to various types of time delay systems. The following theorem simply summarizes stability results on the system by noting that the current system is of retarded type.

Theorem 1. (Cheong et al., 2005) For the closed loop system with characteristic function (5), there exists a constant $R_{MAD}>0$ such that (i) the closed loop system is bounded stable if $0<R<R_{MAD}$, and (ii) $|x_1-x_2|\to 0$ as $t\to\infty$ if $F_1(t)$ and $F_2(t)$ are transient and damping coefficient is nonzero. ■

Remark 2.1 Even to a step inputs, $F_1(t)$ and $F_2(t)$, the state difference, $|x_1-x_2|$, in the steady state, can become zero whenever the delay condition is symmetric, i.e., $T_1=T_2$; otherwise, it is bounded.

So far, we have assumed that every parameter in the system is known, which is quite a restrictive condition to deal with physical plants. In case when uncertainty is not negligible, system's stability should be re-tested after incorporating conditions of uncertainties. There are two kinds of uncertainties conceivable in the system under consideration. They are: (i) uncertainty in the amount of delay and (ii) uncertainty in the plant model. Although the two uncertainties usually go together, we will isolate them as independent sets so as to clearly present individual effects. In the next section, we provide a way to analyze robust stability under the uncertainties and find a family of system models which guarantees stability.

3. Robustness Analysis for Second-Order Uncertainties

We may confront with second-order or higher-order uncertainties which are not in the definition of conventional single additive or multiplicative uncertainties when identical subsystems are connected just like the one in Fig. 2. When two identical subsystems are involved, the uncertain fractions of the subsystems are multiplied, yielding a second-order polynomial with respect to the uncertainty fraction. If we model these higher-order uncertainties in a conventional single-order lumped uncertainty, we may loose a chance to finely tune the corresponding robust boundary. So, this section is devoted to robustness analysis for the systems having a second-order uncertainty.

3.1 Robust bound of delay uncertainty

Since time delay possibly changes from the nominal value and may not be measured precisely in practice, we need to see the closed loop behavior when there is a delay mismatch. We first define the delay mismatch by $\delta R := R_n - R$, where

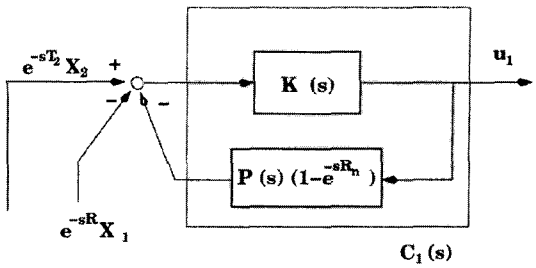

(a) Case of $R_n \neq R$ and $P_n(s)=P(s)$

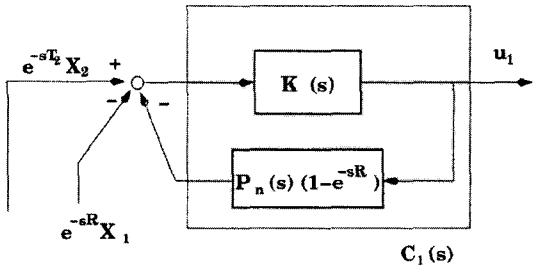

(b) Case of $R_n=R$ and $P_n(s) \neq P(s)$

Fig. 4 Two cases of controller $C_1(s)$ (It is the same for $C_2(s)$ by the symmetry.)

R_n is the nominal delay that is the best known value of actual R. As depicted in Fig. 4(a), since the internal model in the controller utilizes R_n instead of real R, the equation in (2) is modified as:

$$u_i=\frac{K(s)}{1+K(s)P(s)(1-e^{-sR_n})}(X_j e^{-sT_j}-X_i e^{-sR}) \quad (6)$$

and by combining (6) and (3), a modified transfer relation is obtained with the following characteristic function:

$$\begin{aligned}&\varphi_d(s, R; \delta R)\\ &=a_2(s)e^{-2\delta Rs}+a_1(s)e^{-\delta Rs}+a_0(s)\end{aligned} \quad (7)$$

where

$$a_2(s)=K^2(s)e^{-2Rs}$$

$$a_1(s)=-2K(s)(M(s)+K(s))e^{-Rs}-2K^2(s)e^{-2Rs}$$

$$\begin{aligned}a_0(s)=&(M^2(s)+2K(s)M(s)+K^2(s))\\ &+(2K(s)M(s)+K^2(s))e^{-Rs}\end{aligned}$$

$$M(s):=P^{-1}(s)=ms^2+bs$$

This is a characteristic function where quasi-polynomial, $a_i(s)$, $i=1, \cdots, 3$ is multiplied by commensurate delay mismatch, $e^{\delta R}$. If $\delta R=0$,

$\varphi_d(s, R; \delta R)$ simply reduces to $\varphi(s, R)$. Note that (7) is a second order algebraic polynomial with respect to $e^{-\delta Rs}$. This is a result from combining two identical subsystems. We call $\varphi_d(s, R; \delta R)$ an uncertainty characteristic polynomial with respect to $e^{-\delta Rs}$.

Definition 1. The system with characteristic equation in (7) is practically stable with respect to δR, when there exists a bound $B(\delta R)$ such that roots of (7) are all in the left half plane for every $\delta R \in B(\delta R)$.

By factorizing (7), two kinds of solutions of $\varphi_d(s, R; \delta R)=0$ for $e^{-\delta Rs}$ are obtained as follows after some algebraic manipulation.

$$e^{-\delta Rs}=\left(\frac{M(s)}{K(s)}+1\right)e^{Rs}+e^{Rs/2s}+1 \text{ and}$$
$$e^{-\delta Rs}=\left(\frac{M(s)}{K(s)}+1\right)e^{Rs}-e^{R/2s}+1 \tag{8}$$

In order to compute the stable bound $B(\delta R)$, the first step to take is to compute imaginary roots of (8), since they represent crossing points between stable and unstable domains. The imaginary roots are obtained by substituting $j=jw$ into the magnitude relation of (8) as follow.

$$1=\left|\left(\frac{M(jw)}{K(jw)}+1\right)e^{jwR}+e^{jwR/2}+1\right| \text{ and}$$
$$1=\left|\left(\frac{M(jw)}{K(jw)}+1\right)e^{jwR}-e^{jwR/2}+1\right| \tag{9}$$

As can be seen, the amount of delay mismatch has nothing to do with computing the crossing frequencies. For clarity of notation, crossing frequencies from the first part in the above are denoted by $w=w_i$, $i=1, 2, \cdots, m$, and those from the second part are denoted by $w=w_l$, $l=1, 2, \cdots, n$. These are obtained through sweeping w from zero to infinity and selecting values that satisfy the above magnitude conditions (Michiels and Niculescu, 2003). An interesting fact is that for given R, there are only finite imaginary roots. This can be simply conjectured by using the bilinear transform proposed by Thowsen (Thowsen, 1981) as

$$e^{-Rs}=\left(\frac{1+T_s}{1-Ts}\right)^2\Big|_{s=jw}$$

where T is a constant that is directly related to delay R. If we apply this relation into (9), we obtain a new polynomial equation with finite order, which means the number of imaginary roots of (9) are finite, yielding a finite number of roots.

After finding the crossing frequencies, next is to determine the bound of δR for which system keeps stability, using phase angle condition of (8). Applying the phase angle condition to (8), we get conditions of δR that are consistent with the imaginary roots as follows.

$$\delta R_{ik}^{(1)}=\frac{-2k\pi}{w_i}-\frac{1}{w_i}\angle\left[\left(\frac{M(jw_i)}{K(jw_i)}+1\right)e^{jRw_i}+e^{jRw_i/2}+1\right] \tag{10}$$

and

$$\delta R_{lk}^{(2)}=\frac{-2k\pi}{w_l}-\frac{1}{w_l}\angle\left[\left(\frac{M(jw_l)}{K(jw_l)}+1\right)e^{jRw_l}+e^{jRw_l/2}+1\right] \tag{11}$$

where k is any integer, and the superscript (i), $i=1, 2$, explicitly denotes that the term is related to the i-th case in (8). The above equation implies that at each crossing frequency, $s=jw_i$ or $s=jw_l$, an infinite number of crossovers between left and right half complex planes occurs as δR varies.

Theorem 2. Practical stability of the system with characteristic equation given in (7) is guaranteed for delay mismatch $\delta R \in B(\delta R)$ with $B(\delta R)$ given by

$$B(\delta R)=\{\delta R \,|\, \max(\delta R_{\max}^{-}, -R) \le \delta R < \delta R_{\min}^{+}\} \tag{12}$$

where $\delta R_{\min}^{+}$ and $\delta R_{\max}^{-}$ are minimum positive and maximum negative constants among the values that satisfy (10) or (11).

Proof. The considered system, initially stable when δR is zero, becomes unstable as δR is increased or decreased beyond a certain bound. Just before the system becomes unstable, some poles of it must pass through the imaginary axis. These poles must belong to the sets of jw_i or

jw_l obtained by Eq. (9), and each imaginary pole determines the possible values of δR via relations (10) or (11). Among such values of δR, the minimum positive of δR, that is, $\delta R^{+}_{\min}$, yields the first crossover as δR is increased from zero to positive infinity. Similarly, the maximum negative of δR, that is, $\delta R^{-}_{\max}$, yields the first crossover as δR is decreased from zero to negative infinity. Hence, by the assumption that the characteristic equation is stable for $\delta R=0$, the first touchdowns of roots to the imaginary axis, as δR varies in the negative and positive directions, imply the lower and the upper stable bounds of δR. Thus, defining $\delta R^{-}_{\max}$ and $\delta R^{+}_{\min}$ as the maximum negative and the minimum positive values among the combined set of $\delta R^{(1)}_{i,k}$ and $\delta R^{(2)}_{l,k}$ for every i, k, and l, we can obtain robust bound of $B(\delta R)$. Furthermore, since nominal delay, R_n, takes only positive values, additional condition to be met is $\delta R \geq -R$. Therefore, every δR in the bound $B(\delta R)$ in (12) satisfies the stability condition of characteristic function (7). ■

Numerical example 1. This example demonstrates how to compute the robust bound of $B(\delta R)$. We consider a plant, $P(s)=1/(s^2+0.2s)$ and two choices of controllers, i.e., $K(s)=2s+2$ and $K(s)=5s+20$. For each controller, we compute crossing frequencies and delay uncertainty bound as shown in Figs. 5 and 6.

For this purpose, using (9) the crossing frequencies, w_i and w_l, are determined as a function of R for both cases of controllers and plotted in Figs. 5(a) and 6(a). From the figures, we can verify that if tuple (w_i, R) is a solution, then so is $(w_i, R+2\pi k/w_i)$, $k \in Z^+$, which can also be mathematically verified by combining relations in (8) and (9). Also note that the crossing frequencies tend to increase as the controller gains are getting larger.

Using the computed crossing frequencies and the equations in (10) and (11), we get $\delta R^{-}_{\max}$ and $\delta R^{+}_{\min}$, and consequently the corresponding robust delay margin $B(\delta R)$ as shown in Figs. 5(b) and 6(b). In the figures, $B(\delta R)$ is wider for small values of R and reduces substantially for large

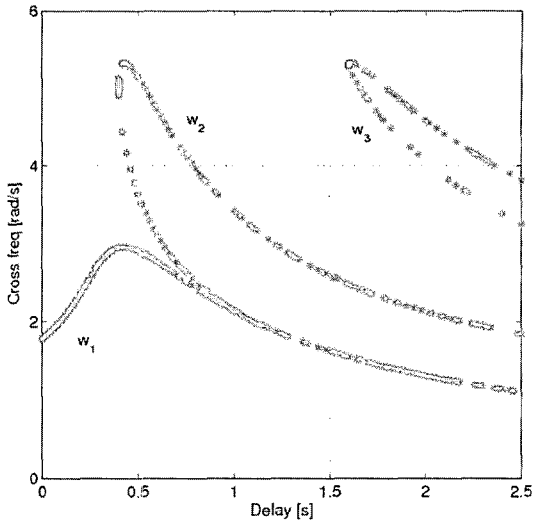

(a) Crossing frequencies

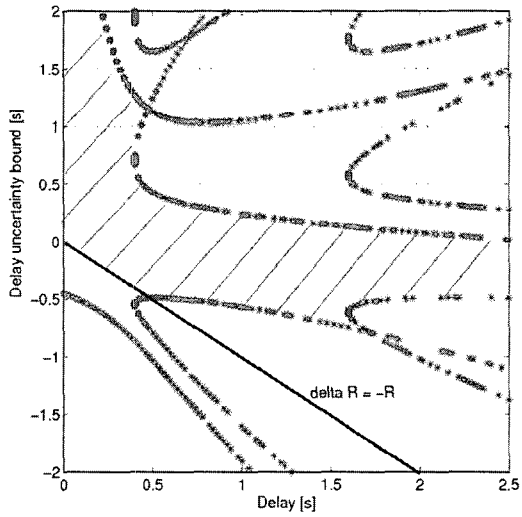

(b) Delay uncertainty bound, $B(\delta R)$

Fig. 5 Crossing frequencies and delay uncertainty bound ($k_v=2$, $k_p=2$)

values of R. Comparing both cases of controllers, we find out that higher controller gains shrink robust delay bound significantly although it may improve synchronization capability up to certain values. Further increase of controller gains pushes some of poles near to the imaginary axis, which results in poor control performance. Note that the ranges of horizontal axes between Figs. 5 and 6 are different. This is because the maximum allowable delays, R_{MAD}, for the two cases are around 2.5s and 0.63s, respectively, and it is not necessary

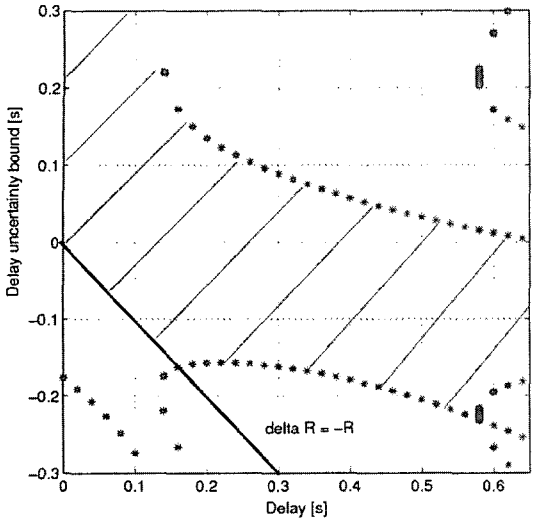

(a) Crossing frequencies

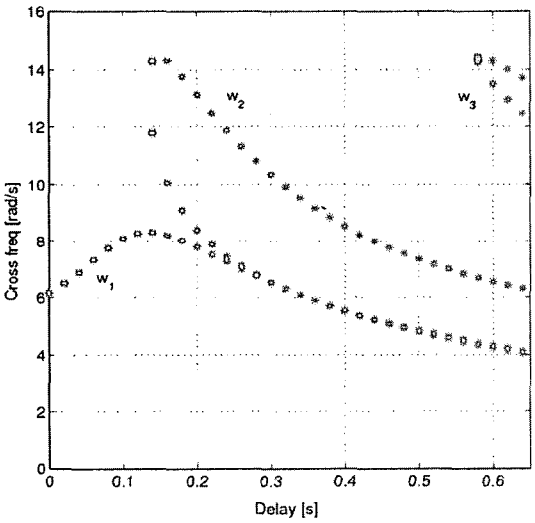

(b) Delay uncertainty bound, $B(\delta R)$

Fig. 6 Crossing frequencies and delay uncertainty bound (k_v=5, k_p=20)

to consider delay values beyond the nominal stability limit.

3.2 Robust bound of plant uncertainty

For the case when the controller utilizes $P_n(s)$, different from $P(s)$, as shown in Fig. 4(b), stability is possibly affected by the amount of plant mismatch. To deal with this problem, we first define plant deviation as $\Delta(s) := P(s) - P_n(s)$, while the amount of delay is assumed to be exact such that $R_n = R$ to focus on the pure effect of plant uncertainty to the stability. In the subsequent analysis, we provide a way to determine a tolerable amount of $\Delta(s)$, for which stability is guaranteed, and the corresponding geometrical meaning is given as well.

Here we further assume that the structure of plant dynamics is known in advance. That is, for $P(s) = 1/(ms^2 + bs)$, its model can be estimated as $P_n(s) = 1/(m_0 s^2 + b_0 s)$. The condition of exactly known constant delay might be rather strict in regards to modern network behavior, but it is certainly achievable by using a simple buffering technique with a cost of increased time delay. For example, as addressed by Kosuge et al. (1996) statistically known maximal delay value is set as the artificial constant delay value by holding actual data delivered earlier than by the maximal delay value until the artificial delay value is met.

Employing the controller with plant uncertainty shown in Fig. 4(b), we have a modified characteristic function as follows.

$$\varphi_p(s, R; q) = c_2(s) + c_1(s)\, q(s) + c_0(s)\, q^2(s) \quad (13)$$

where $q(s) := P_n(s)/P(s)$ and

$$c_2(s) = K^2(s)\, e^{-2Rs} + K(s)\{2M(s) - K(s)\}\, e^{-Rs} + M^2(s)$$
$$c_1(s) = -2K^2(s)\, e^{-2Rs} - 2K(s)\{M(s) - K(s)\}\, e^{-Rs} + 2K(s)\, M(s)$$
$$c_0(s) = K^2(s)\, e^{-2Rs} - 2K^2(s)\, e^{-Rs} + K^2(s)$$

Eq. (13) shows the characteristic function is a second-order rational polynomial with respect to $q(s)$. Thus, similarly, we call $\varphi_p(s, R; q)$ an uncertainty characteristic polynomial with respect to $q(s)$.

If $q(s) \equiv 1$, implying $P_n(s) \equiv P(s)$, the characteristic function $\varphi_p(s, R; q)$ reduces to $\varphi(s, R)$. Since $q(s)|_{s=jw} \equiv 0 \forall w \in Re$ implies a trivial solution, we may rewrite the form of $\varphi_p(s, R; q)$ as

$$\varphi_p(s, R; q) = q^2(s)\{c_2(s)\, q^{-2}(s) + c_1(s)\, q^{-1}(s) + c_0(s)\} \quad (14)$$

which makes a second-order polynomial with respect to $q^{-1}(s)$ with rational coefficients, $c_i(s)$. As defined in the previous section, the amount of uncertainty can be written as

$$q^{-1}(s)=\frac{P(s)}{P_n(s)}=1+\delta(s) \tag{15}$$

where $\delta(s):=\Delta(s)/P_n(s)$ is the normalized amount of uncertainty in the plant. There are two kinds of solutions to $\varphi_p(s, R; q)$ as follows.

$$\lambda_1(s)=\frac{-c_1(s)+\sqrt{c_1^2(s)-4c_2(s)c_0(s)}}{2c_2(s)} \text{ and}$$
$$\lambda_2(s)=\frac{-c_1(s)-\sqrt{c_1^2(s)-4c_2(s)c_0(s)}}{2c_2(s)} \tag{16}$$

for $c_2(s)\neq 0$. If we plug $s=jw$ into the solutions, $\lambda_1(jw)$ and $\lambda_1(jw)$ become the loci pertaining all the imaginary roots that are on the stability boundary. Hence, in order for the system to be stable, the following relation must be satisfied:

$$|q^{-1}(jw)-\lambda_1(jw)|\neq 0, \text{ and}$$
$$|q^{-1}(jw)-\lambda_2(jw)|\neq 0, \ \forall w\in Re \tag{17}$$

Substituting (15) into (17) yields

$$|\delta(jw)-\bar{\lambda}_1(jw)|\neq 0, \text{ and}$$
$$|\delta(jw)-\bar{\lambda}_2(jw)|\neq 0, \ \forall w\in Re \tag{18}$$

where $\bar{\lambda}_i=\lambda_i-1$, $i=1, 2$. Because the system is stable when $\delta(jw)=0$, Eq. (18) is identical to inequalities:

$$|\delta(jw)|<|\bar{\lambda}_1(jw)|, \text{ and}$$
$$|\delta(jw)|<|\bar{\lambda}_2(jw)|, \ \forall w\in Re \tag{19}$$

Two classes of stability bound for $\delta(jw)$ can be defined: (i) frequency independent bound; and (ii) frequency dependent bound. The frequency independent bound is a tolerable uncertainty bound determined by the maximum disk centered at the origin such that

$$B_c(\delta(\delta w))=\{\delta(jw)| \ |\delta(jw)|<\rho\} \tag{20}$$

where $\rho=\min_{i=1,2,\ \forall w\in Re}(|\bar{\lambda}_i(jw)|)$.

The above frequency independent bound satisfies inequality in (19) but is sometimes too conservative. Fig. 7(a) shows a schematic of frequency independent bound for $\delta(jw)$. Since the disk represents a very limited region around the origin, the plant model, $P_n(s)$, must restrictively be very close to the actual plant dynamics, $P(s)$.

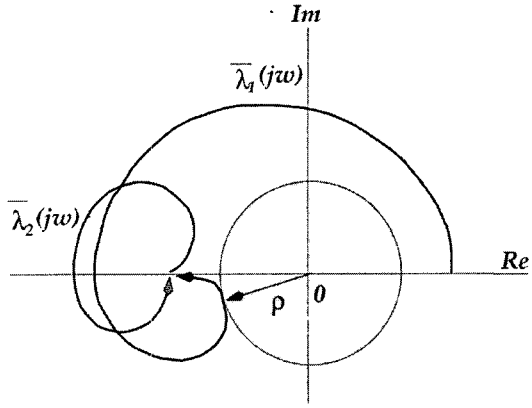

(a) Frequency independent bound

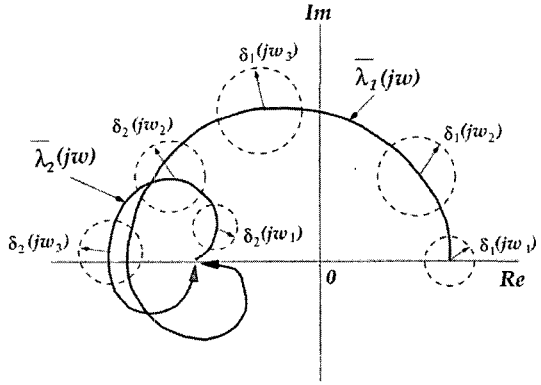

(b) Frequency dependent bound

Fig. 7 Two definitions of plant uncertainty bound

Also the dynamic structures between the model and the plant should be exactly the same. For example, only if $P(s)$ and $P_n(s)$ have the same form such that $P(s)=1/(ms^2+bs)$ and $P_n(s)=1/(m_0s^2+b_0s)$, the normalized model deviation, $\delta(jw)=\{(m_0-m)s^2+(b_0-b)s\}/(ms^2+bs)$, has values inside the disk at extreme frequencies such that

$$|\lim_{w\to 0}\delta(jw)=(b_0-b)/b|<\rho \text{ and}$$
$$|\lim_{w\to\infty}\delta(jw)=(m_0-m)/m|<\rho.$$

Otherwise, $\delta(jw)$ does not reside in the disk.

On the other hand, the frequency dependent bound provides a more realistic measure of uncertainty, allowing an exact uncertainty bound along the frequency variation. It is represented as a single inequality as follows, by combining two inequalities in (19).

$$B_p(\delta(jw))=\{\delta(jw)|\ |\delta(jw)|<\min(|\bar{\lambda}_1(jw)|, |\bar{\lambda}_2(jw)|), \forall w\in Re\} \quad (21)$$

Since the magnitude of $\bar{\lambda}_i(jw)$ is varying as a function of frequency, so is the frequency dependent bound. Geometrically, as shown in Fig. 7 (b), the frequency dependent bound implies the maximum radius of a circle along the loci of $\bar{\lambda}_i(jw)$, $i=1, 2$ which is smaller than the distance from the origin to the point of the circle center.

Numerical example 2. In order to demonstrate how to determine the robust bound of $\delta(jw)$, we take two examples with two different sets of primary controller gains ; that is, (1) $K(s)=2s+2$, and (2) $K(s)=5s+20$, just the same as the numerical example 1 in the previous subsection. The dynamics of plant is $P(s)=1/(s^2+0.2s)$, and time delay is set to $R=0.3$s. For both cases of controllers, the corresponding loci of $\bar{\lambda}_1(jw)$ and $\bar{\lambda}_2(jw)$ $\forall w>0$ are shown in Fig. 8 using the formula in Eq. (16).

After scanning the magnitudes of $\delta(jw)$, we find out that frequency independent robust bounds of $\delta(jw)$ are disks centered at the origin with radii $\rho=0.86$ and $\rho=0.48$ for the two cases, respectively. (The larger gain tends to shrink robust bound in general.) Sometimes it is favorable to know the frequency independent robust bound of $q(jw)$, rather than that of $\delta(jw)$ or $q^{-1}(jw)$. This is easily derived as follows. Since $|\delta(jw)|=|q^{-1}(jw)-1|<\rho$, we have

$$|q(jw)-1|<\rho|q(jw)|,\ (\rho<1) \quad (22)$$

which is again a disk in the complex plane as

$$|q(jw)-q_0|<\rho/(1-\rho^2) \quad (23)$$

where $q_0=1/(1-\rho^2)$. For the case of $\rho=086$, the disk representing the robust bound of $q(jw)$ is centered at $3.84+0j$ with radius of 3.30.

The plots of frequency dependent margins are given in Fig. 9 along with frequency axis for the two cases. The minimum value of $\bar{\lambda}_i=\lambda_i-1$, $i=1, 2$ is the frequency independent margin of $\delta(jw)$. Assuming $P_n^{-1}(s)=M_n(s)=m_0s^2+b_0s$, we have $\delta(s)=[(m_0-1)s^2+(b_0-0.2)s]/(s^2+0.2s)$. In the first case shown in Fig. 9(a), the

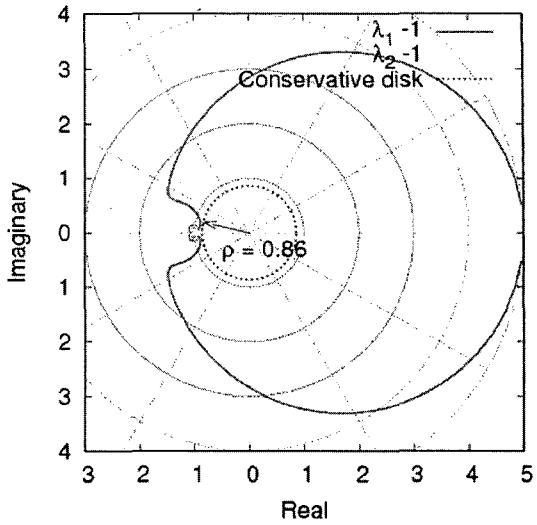

(a) $K(s)=2s+2$

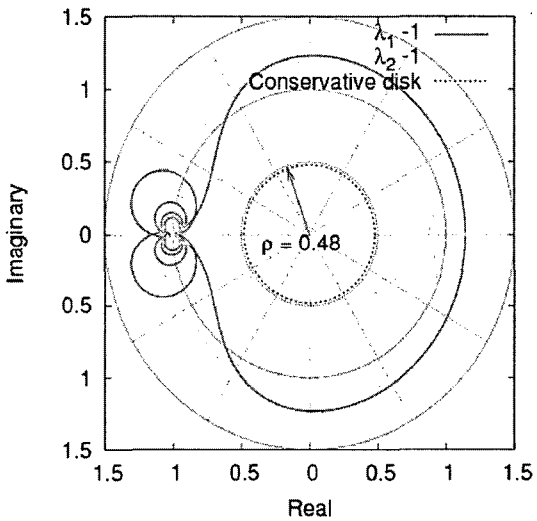

(b) $K(s)=5s+20$

Fig. 8 Frequency independent bound of plant uncertainty when $R=0.3$s

robust bound of $\delta(jw)$ maintains the unity value around the zero and the infinite frequencies but drops a little to 0.86 at $s=14.17j$. These conditions yield

$$\begin{aligned}&\text{(a) } \lim_{s\to 0}|\delta(jw)|=|b_0-0.2|\le 0.2,\\ &\text{(b) } \lim_{s\to\infty}|\delta(jw)|=|m_0-1|\le 1, \text{ and}\\ &\text{(c) } |\delta(14.17j)|\le 0.86\\ &\quad\rightarrow \frac{(m_0-1)^2}{0.856^2}+\frac{(b_0-0.2)^2}{12.14^2}<1\end{aligned} \quad (24)$$

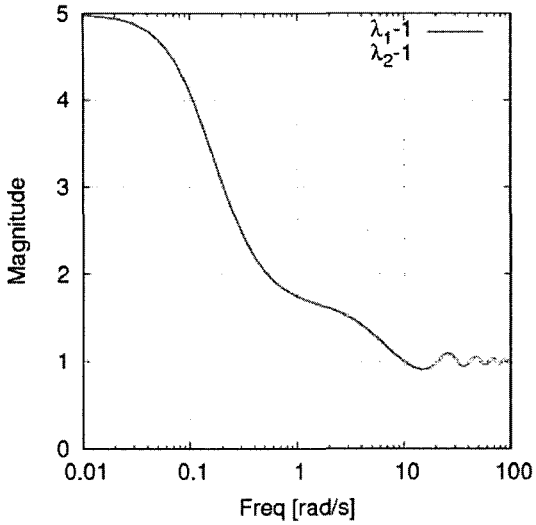

(a) $K(s)=2s+2$

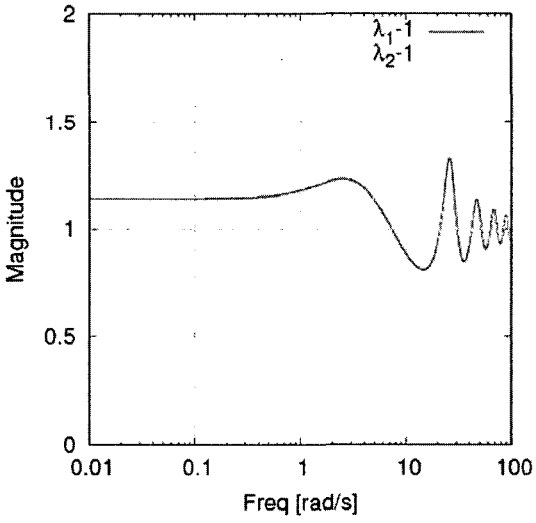

(b) $K(s)=5s+20$

Fig. 9 Frequency dependent bound of plant uncertainty when $R=0.3$s

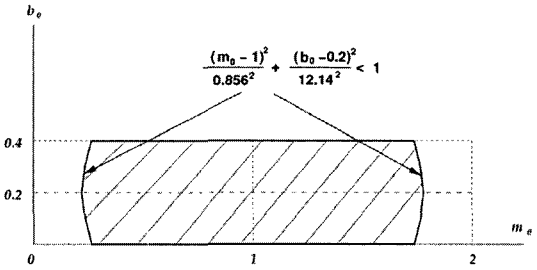

(a) $K(s)=2s+2$

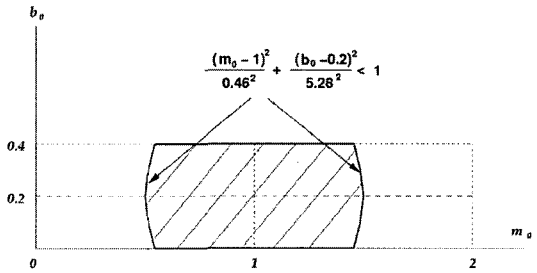

(b) $K(s)=5s+20$

Fig. 10 Uncertainty bound in parameter space

$$\text{(a)}\ \lim_{s\to 0}|\delta(jw)|=|b_0-0.2|\le 0.2,$$

$$\text{(b)}\ \lim_{s\to\infty}|\delta(jw)|=|m_0-1|\le 1,\ \text{and} \tag{25}$$

$$\text{(c)}\ |\delta(11.0j)|\le 0.48 \rightarrow \frac{(m_0-1)^2}{0.48^2}+\frac{(b_0-0.2)^2}{5.2808^2}<1$$

which are graphically depicted in Fig. 10(a). So approximately any choice of the parameter pair (m_0, b_0) inside the region guarantees the robust stability. For the second case, the robust bound of $\delta(jw)$ is unity up to around $w=2$ but drops down to 0.48 at $w=11$, which is smaller than that of the first case. See Fig. 9(b). Now repeating the same procedures, we can approximate a region of parameter pairs for robust stability defined by the relations:

which are graphically given in Fig. 10(b). In this case, the robust region is narrowed very much compared to that of the first case. Conclusively, while the magnitude of controller gain may help expedite the synchronization, it tends to reduce robust bounds not only of the delay uncertainty but also of the plant uncertainty. So, we may have to negotiate the performance and stability to a suitable point.

Remark 3.1 As mentioned at the beginning of this section, for the most general cases, two uncertain factors, δR and $\delta(s)$ must be treated at the same time. Unfortunately the relation between δR and $\delta(s)$ is nonlinear and complex, and finding both bounds with one numerical procedure is also another huge research topic. So, as a tentative technique, we introduce brief numerical procedures that roughly guide how to find both uncertainty bounds in general mixed cases by

extending section 3.2.

For general cases, $c_0(s)$ through $c_2(s)$ of (13) possess delay uncertainty, $e^{-s\delta R}$. First, fix δR to small number, say $\gamma_0>0$. Then perform the frequency sweeping method as was done in Numerical Example 2. This gives uncertainty bound $\delta(s)$ for $\delta R=\gamma_0$. Increase γ_0 to γ_1 and repeat the frequency sweeping method to find $\delta(s)$ for $\delta R=\gamma_1$. Ultimately, repetition of these numerical procedures can yield uncertainty bounds of $\delta(s)$ and δR simultaneously, even though it consumes much time and energy.

4. Simulation Verification

In order to verify the theoretical results on the robustness analysis in the previous section, we carry out time-based simulations. The dynamics of the considered system is $P(s)=1/(s^2+0.2s)$, which has been utilized throughout the examples in section 3. The primary controller is chosen as $K(s)=5s+20$. We assume that the communication delay is symmetrically given such that $T_1=T_2=0.15$s, which makes $R=0.3$s. The inputs to the system are set to $F_1(t)=\sin(t)$ and $F_2(t)=-\sin(0.4t+1)$.

4.1 Robustness under delay uncertainty

For the given conditions, that is, $K(s)=5s+20$ and $R=0.3$, the robust bound of is estimated approximately as 0.08s by referring to the chart in Fig. 6. To check if it is a good estimation, we run the simulation for two cases of $\delta R=0.05$s ($R_n=0.35$s) and $\delta R=0.09$s ($R_n=0.39$s), one of which is within the robust delay bound and the other is not. As shown in Fig. 11, if δR is chosen to be smaller than the robust margin, the closed loop system is stable, and otherwise, it is unstable. Under the given controller gains, if the maximum allowable delay margin is not sufficient enough to cover the possible amount of delay mismatch in practice, then the controller gains need to be reduced so as to warrant a sufficient robust delay margin.

4.2 Robustness under plant uncertainty

To test the correctness of the computed robust

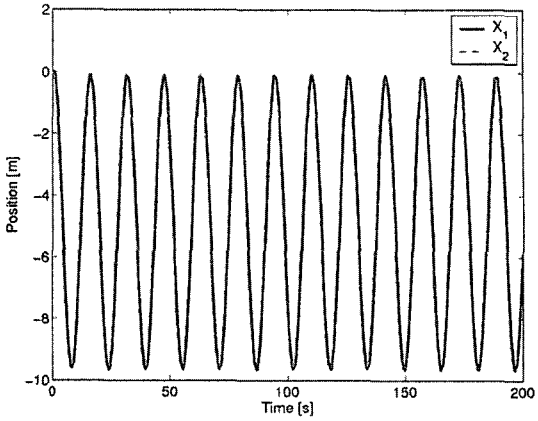

(a) $\delta R=0.05$s

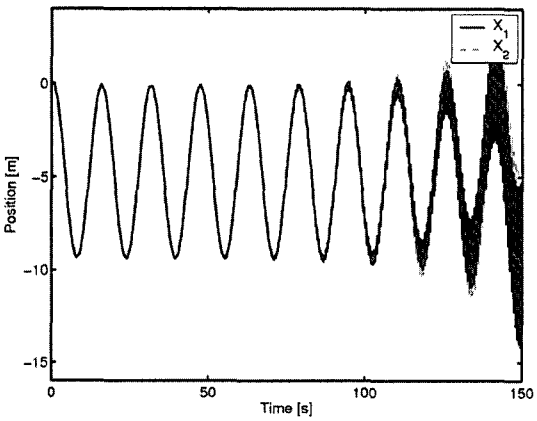

(b) $\delta R=0.09$s

Fig. 11 Simulation result under delay uncertainty

plant uncertainty bound, choose a plant model, $P_n(s)=1/(m_0s^2+b_0s)$, with two parameter pairs as

$$(1)\ (m_0,\ b_0)=(1.0,\ 0.35)\Rightarrow\delta(s)=\frac{0.15s}{s^2+0.2s},$$

$$(2)\ (m_0,\ b_0)=(1.0,\ 0.45)\Rightarrow\delta(s)=\frac{0.25s}{s^2+0.2s},$$

where the first parameter pair is inside the robust bound, while the second parameter pair is outside the robust bound. (Refer to Fig. 10(b)) Since m_0 is equal to true value and only b_0 has a deviation from true value, a possible violation of the robust region occurs in the low frequency region. In the first case, because $\lim_{w\to0}|\delta(jw)|=0.75$, the chosen plant model is in the robust region. But the second case is not in the robust region since $\lim_{w\to0}|\delta(jw)|=1.25$. Simulation re-

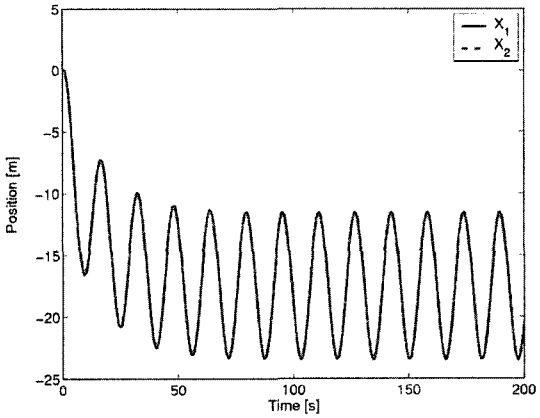

(a) $m_0=1$, $b_0=0.35$

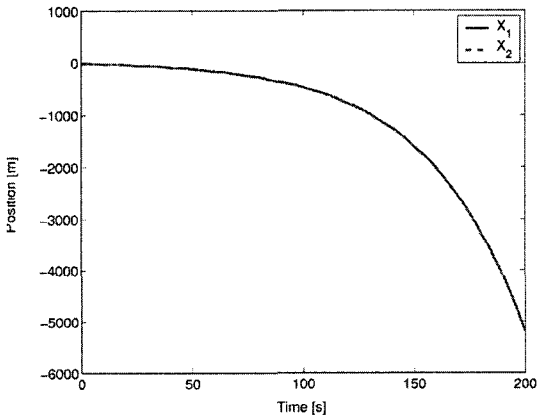

(b) $m_0=1$, $b_0=0.45$

Fig. 12 Simulation result under plant uncertainty

ults in Fig. 12 show clear comparison between the two cases. As expected, the first parameter pair presents a well-synchronized bounded behavior, whereas the second parameter pair shows an unbounded result.

5. Summary and Concluding Remarks

In this paper we presented robustness analysis for a coupled dynamic system having identical subsystems under the control of synchronization feedback scheme. Time delay was included in the model to signify the effect of the data communication.

We defined two possible uncertainties occurred in the considered control structure; that is, the uncertainties in the amount of delay and the plant parameters. Because all subsystems contained in the coupled system are identical, those uncertainties appear in the characteristic function, and we can arrange it in the descending order of the uncertainty parameter. So it is a higher-order polynomial with respect to the uncertainty variable. We particularly focused on the second-order case, where two identical subsystems are involved. For this case, delay and plant uncertainty bounds were explicitly calculated by solving the second-order characteristic polynomials.

The robust delay bound was defined using the minimum positive and maximum negative values of delay uncertainty, for which the characteristic root touches the imaginary axis for the first time as the delay uncertainty is varied from zero to positive and negative directions. As the controller gains and the amount of delay increase, the allowable delay uncertainty tends to decrease. The robust bound for plant uncertainty was classified by the two definitions: frequency independent bound and frequency dependent bound. The former is a conservative bound that is defined in the form of a disk region, while the latter is more accurate bound which provides maximal allowable uncertainty along the frequency variation. For the system represented by a mass with damping resistance, we quantitatively illustrated how to obtain the uncertainty bound in the parameter space. And the analyzed results were confirmed by numerical simulations.

We believe this paper contributes to formulating and analyzing robustness issues in a coupled system with identical subsystems. Though only a simple dynamic system has been considered in the article, the strategic method addressed here is modifiable and applicable to general systems and, thus, can be a ground tool for similar researches.

Acknowledgments

This research was supported by the Korea Research Foundation Grant (KRF-2005-003-D00104)

References

Anderson, R. J. and Spong, M. W., 1989, "Bi-

lateral Control of Teleoperators with Time Delay," *IEEE Trans. on Automatic Control*, Vol. 34, No. 5, pp. 494~501.

Bellman, R. and Cooke, K. L., 1963, *Differential-Difference Equations*, Academic Press.

Changhong, W., Lixian, Z. and Qiyong, W., 2004, "Controller Design Based on Model Predictive Control for Real-Time Tracking Synchronization in Closed-Loop Control Via Internet," *in Proc. of IEEE Int. Conf. on Control Applications*, pp. 260~265.

Cheong, J., Niculescu, S.-I., Annaswamy, A. and Srinivasan, M. A., 2005, "Motion Synchronization in Virtual Environments with Shared Haptics and Large Time Delays," in *Proc. of Symp. on Haptic Interfaces for Virtual Environment and Teleoperator Systems*, pp. 277~282.

Kazerooni, K., Tsay, T. and Hollerbach, K., 1993, "A Controller Design Framework for Telerobotic Systems," *IEEE Trans. on Control System Technology*, Vol. 1, No. 1, pp. 50~62.

Kosuge, K., Murayama, H. and Takeo, K., 1996, "Bilateral Feedback Control of Tele-Manipulators Via Computer network," in *Proc. of IEEE/RSJ Int. Conf. on Intelligent Robots and Systems*, pp. 1380~1385.

Lawrence, D. A., 1993, "Stability and Transparency in Bilateral Teleoperation," *IEEE Trans. on Robotics and Automation*, Vol. 9, pp. 624~637.

Liu, H. H. T. and Sun, D., 2005, "Uniform Synchronization in Multi-axis Motion Control," in *Proc. of American Control Conference*, pp. 4537~4542.

Lung, G. M. H., Francis, B. A. and Apkarian, J., 1995, "Bilateral Controller for Teleoperators with Time Delay Via-Synthesis," *IEEE Trans. on Robotics and Automation*, Vol. 11, No. 1, pp. 105~116.

Michiels, W. and Niculescu, S. -I., 2003, "On the Delay Sensitivity of Smith Predictors," *Int. J. of Systems Science*, Vol. 34, pp. 543~551.

Niculescu, S. -I., 2001, Delay Effects on Stability: A Robust Control Approach. Springer.

Niemeyer, G. and Slotine, J. -J. E., 1991, "Stable Adaptive Teleoperation," *IEEE Journal of Oceanic Engineering*, Vol. 16, No. 1, pp. 152~162.

Rodriguez-Angeles, A. and Nijmeijer, H., 2004, "Mutual Synchronization of Robots via Estimated State Feedback: A Cooperative Approach," *IEEE Trans. on Control Systems Technology*, Vol. 12, pp. 542~554.

Satacesaria, C. and Scattolini, R., 1993, "Easy Tuning of Smith Predictor in Presence of Delay Uncertainty," *Automatica*, Vol. 29, pp. 1595~1597.

Smith, O. J. M., 1957, "Closer Control of Loops with Dead Time," *Chem. Eng. Prog.*, Vol. 53, No. 5, pp. 217~219.

Sun D. and Feng, G., 2003, "A Synchronization Approach to the Mutual Error Control of a Mobile Manipulator," in *Proc. of the IEEE Int. Conf. on Robotics and Automation*, pp. 3005~3010.

Sun, H. and Chiu, G. T. -C., 2002, "Motion Synchronization for Dual-Cylinder Electrohydraulic Lift Systems," *IEEE/ASME Trans. on Mechatronics*, Vol. 7, pp. 171~181.

Taoutaou, D., Niculescu, S. -I. and Gu, K., 2003, "Robust Stability of Teleoperation Schemes Subject to Constant and Time-Varying Communication Delays," in *Proc. of IEEE Conf. on Decision and Control*, pp. 5579~5584.

Thowsen, A., 1981, "An Analytic Stability Test for a Class of Time-Delay Systems," *IEEE Trans. on Automatic Control*, Vol. AC26, No. 3, pp. 735~736.

Walton, K. and Marshall, J. E., 1987, "Direct Method for tds Stability Analysis," *EE Proceedings : Part D*, Vol. 2, No. 2, pp. 101~107.

Yamanaka, K. and Shimemura, E., 1987, "Effects of Mismatched Smith Controller on Stability in Systems with Time-Delay," *Automatica*, Vol. 23, No. 6, pp. 787~791.

Zhang, W. and Xu, X., 2001, "Analytical Design and Analysis of Mismatched Smith Predictor," ISA Transactions, Vol. 40, pp. 133~138.